Inorganic Chemistry

pubs.acs.org/IC

Article

Broadband Near-Infrared Luminescence in Garnet $Y_3Ga_3MgSiO_{12}$: Cr^{3+} Phosphors

Lipeng Jiang, Xue Jiang,* Liangliang Zhang, Quansheng Liu, Xiaoyun Mi, Zhan Yu, Guocai Lv, and Yanjing Su*

Cite This: *Inorg. Chem.* 2023, 62, 4220−4226

Read Online

ACCESS | Metrics & More | Article Recommendations | Supporting Information

ABSTRACT: Broadband near-infrared (NIR) phosphors are the critical component of phosphor converted NIR light-emitting diode (LED) light sources. However, there are still a lack of NIR phosphors with excellent external quantum efficiency (EQE) and thermal stability. Here, we report a highly efficient broadband NIR phosphor $Y_3Ga_3MgSiO_{12}$: Cr^{3+}. The optimized phosphor yields an internal quantum efficiency (IQE) and an EQE of 79.9 and 33.7%, respectively. The integrated emission intensity still remains at 84.4% of that at room temperature when heated to 423 K. A broadband NIR LED lamp was made by combining as-prepared phosphor and a blue InGaN LED chip, which shows an output power of 89.8 mW with a photoelectric conversion efficiency of 17.1% driven at 525 mW input power. Our research provides a promising NIR phosphor with high efficiency broadband for the NIR light source.

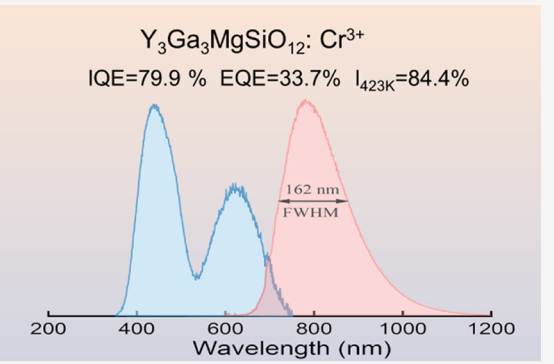

1. INTRODUCTION

Broadband near-infrared (NIR) light sources are playing an important role in brain imaging, palmprint identification, biological sensing, food composition analysis, etc., and are attracting increasing attention.[1−3] However, traditional infrared light sources (e.g., incandescent lamp and tungsten halogen lamp) suffer from the shortcomings of large size, low efficiency, and limited lifespan, which cannot meet the commercial application demands.[4−6] The newly developing NIR light-emitting diodes (LEDs) offer a long service life, high conversion efficiency, and small size, but the full width at half maximum (FWHM) of their emission bands is typically less than 50 nm, limiting their applications.[7,8] Inspired by white LEDs, NIR phosphor converted LEDs (NIR-pc-LEDs) provides a good solution to this problem, which possesses the advantages of compactness, low pollution, long lifetime, and competitive price.[9−12] Moreover, it can be combined with various NIR phosphors to satisfy the demands of potential fields. NIR phosphors act as an essential component of NIR-pc-LEDs. As a result, one of the most difficult issues in promoting the further development of NIR light sources is to produce high emission efficiency and outstanding thermal stable NIR phosphors.[13]

The transition metal Cr^{3+} ion is an ideal NIR luminescence activator as its excitation band matches favorably with the emission band of commercially available blue InGaN LED chips.[2,14] The spectral properties of Cr^{3+} are strongly dominated by the crystal field (CF) environment of the host lattice. Due to the spin forbidden ($^2E_g \rightarrow {}^4A_{2g}$) transition, Cr^{3+} exhibits a narrow sharp line at about 696 nm when it is in a strong CF environment.[15,16] When Cr^{3+} is in a wake CF environment, it exhibits broadband emission at 650−1200 nm, which is associated with the spin-allowed $^4T_{2g} \rightarrow {}^4A_{2g}$ transition.[17−19] After years of research, researchers have reported that Cr^{3+} can emit red and NIR light in many hosts, such as $GdAl_3(BO_3)_4$: Cr^{3+} (broad band, λ_{em} = 740 nm),[20] La_2MgZrO_6: Cr^{3+} (broad band, λ_{em} = 825 nm),[21] $KAlP_2O_7$: Cr^{3+} (broad band, λ_{em} = 790 nm),[22] $LiInSi_2O_6$: Cr^{3+} (broad band, λ_{em} = 840 nm),[23] $Y_3MgAl_3SiO_{12}$: Cr^{3+} (broad band, λ_{em} = 760 nm),[24] etc. Among them, garnet is considered as an excellent host due to its typically large band gap, which can suppress the electron-phonon coupling (EPC) of Cr^{3+} to the host lattice.[25−27] Cr^{3+}-doped garnet NIR phosphors have been widely studied, and a series of high internal quantum efficiency (IQE) and thermal stable NIR phosphors have been reported (Table 2). However, the external quantum efficiency (EQE) of the developed phosphors is usually low, which is essentially due to the low photon-absorbing efficiency of the parity-forbidden d−d transition of Cr^{3+}.[28−31] Discovering broadband NIR phosphors with high EQE is of significant importance for NIR spectroscopic applications.

Received: December 8, 2022
Published: March 1, 2023

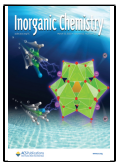

https://doi.org/10.1021/acs.inorgchem.2c04319
Inorg. Chem. 2023, 62, 4220−4226

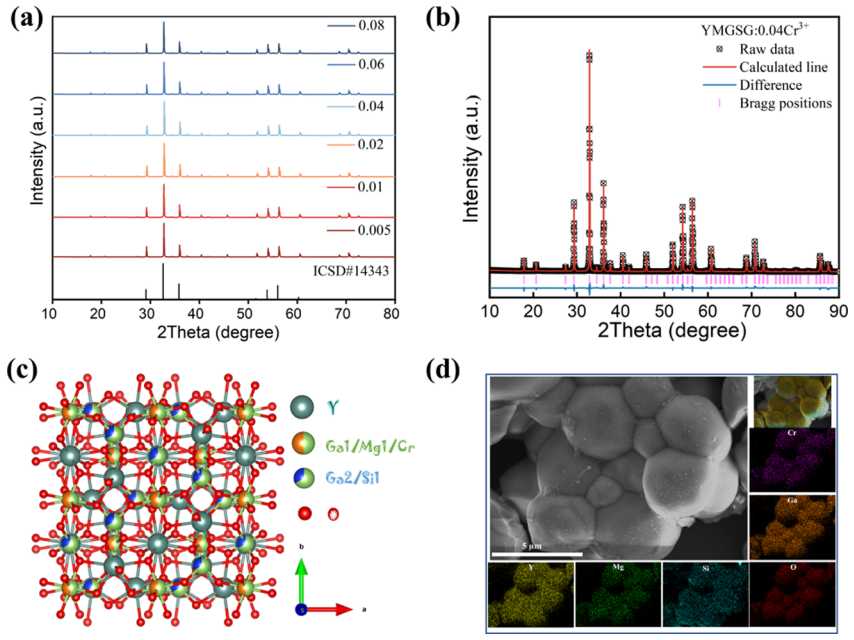

Figure 1. (a) XRD patterns of YMGSG: xCr^{3+} (x = 0.005−0.08). (b) Rietveld refinement XRD pattern of YMGSG: 0.04Cr^{3+}. (c) Crystal structure of YMGSG: 0.04Cr^{3+}. (d) SEM images and elemental mapping of YMGSG: 0.04Cr^{3+}.

In this work, the garnet $Y_3Ga_3MgSiO_{12}$: Cr^{3+} (YMGSG: Cr^{3+}) NIR phosphor is studied in detail, which is obtained by replacing Ga^{3+}−Ga^{3+} with Mg^{2+}−Si^{4+} in the $Y_3Ga_5O_{12}$ garnet structure, where Cr^{3+} occupies the [Ga/MgO$_6$] octahedron. The optimized YMGSG: 0.04Cr^{3+} shows a good thermal stability (84.4%@423 K) attributed to the large band gap (5.61 eV) and the weak coupling of Cr^{3+} with the YMGSG host. Meanwhile, owing to the high blue light absorption efficiency (42.2%), it leads to a high EQE of 33.7% for YMGSG: 0.04Cr^{3+}. The packaged NIR LED device realizes a high output power of approximately 89.8 mW with an input power of 525 mW. These results indicate that YMGSG: 0.04Cr^{3+} phosphor has great potential for spectral applications.

2. MATERIALS PREPARATION AND CHARACTERIZATION

The phosphors were synthesized by the conventional solid-state reaction method. The design of the phosphors follows the chemical formula YMGSG: xCr^{3+} (x = 0.005−0.08). Y_2O_3 (99.99%), Ga_2O_3 (99.99%), MgO (99.99%), SiO_2 (99.9%), and Cr_2O_3 (99.99%) were taken as raw materials. First, the oxides of each component are accurately weighed according to the chemical formula and mixed thoroughly. The mixture was then put in a corundum crucible and heated to 1400 °C in a muffle furnace for 5 h. The desired phosphors are obtained as it cools to room temperature.

The X-ray diffraction spectrum was carried out by the Bruker D8 ADVANCE X-ray diffractometer equipped with a LynxEyeXE-T detector operating at 40 kV and 40 mA. Rietveld refinement was conducted by GSAS software. The diffuse reflection (DR) spectra were collected by a UV−vis−NIR spectrophotometer (PE lambda 750). The photoluminescent excitation (PLE), emission (PL) spectra, thermal quenching properties, and decay curves were collected and recorded by the Edinburgh FLS-1000 fluorescence spectrophotometer. The IQE/EQE was recorded by an absolute PL quantum yield measurement system (Quantaurus-QY Plus C13534-12, Hamamatsu Photonics). The scanning electron microscopy (SEM) images and component elemental maps were measured by Gemini300 equipped with an Oxford accessory. The output power of the prepared LED was measured by the HP8000 LED fast-scan micro-spectrophotocolorimeter (Hopoo Optoelectronics Co., Ltd.). Visible photos were taken by a smartphone, and NIR photos were taken by using a USB NIR camera (Shenzhen Zhongweiaoke Technology Co. Ltd., 1080 P, 700−1100 nm).

3. RESULTS AND DISCUSSION

3.1. Crystal Structure and Morphology. Figure 1a displays the X-ray diffraction (XRD) patterns of YMGSG: xCr^{3+} (x = 0.005−0.08). All the patterns match well with the standard card (ICSD#14343), which means that we obtained the pure garnet phases. To further investigate the crystal structure of as-prepared phosphors, Rietveld refinements were performed as shown in Figure 1b. The results indicate that the crystal structure of YMGSG: Cr^{3+} is cubic, $Ia\bar{3}d$ (no. 230) space group (Table 1). The residual factors are χ^2 = 2.4, R_{wp} = 5.24%, and R_p = 6.87%, respectively, suggesting the reliability of the refined structural model, confirming the prepared phosphor has a pure garnet phase. The atomic positions are listed in Table S1.

Table 1. Crystallographic Data of YMGSG: 0.04Cr^{3+}

x value	x = 0.04
crystal system	cubic
space group	$Ia\bar{3}d$
lattice parameters	
$a/b/c$ (Å)	12.217
$\alpha/\beta/\gamma$ (deg)	90
cell volume (Å^3)	1823.4
R_p	6.87
R_{wp}	5.24
χ^2	2.4

Figure 1c shows the Rietveld refinement crystal structure of YMGSG: 0.04Cr^{3+}. In the cubic garnet crystal, Y, Ga$_{(1)}$Mg, Ga$_{(2)}$Si occupy dodecahedra, octahedra, and tetrahedra respectively. It has been shown that Cr^{3+} (CN = 6, CN: coordination number) has an ionic radius of 0.615 Å, and it prefers to occupy an octahedral position. The SEM image and

https://doi.org/10.1021/acs.inorgchem.2c04319
Inorg. Chem. 2023, 62, 4220−4226

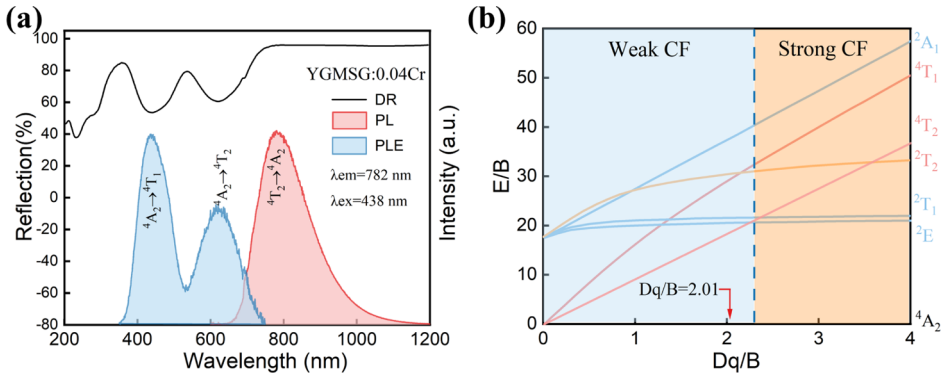

Figure 2. (a) DR, PLE, and PL spectra of YMGSG: 0.04Cr^{3+}. (b) Tanabe−Sugano energy level diagram of Cr^{3+} ions with octahedral coordination.

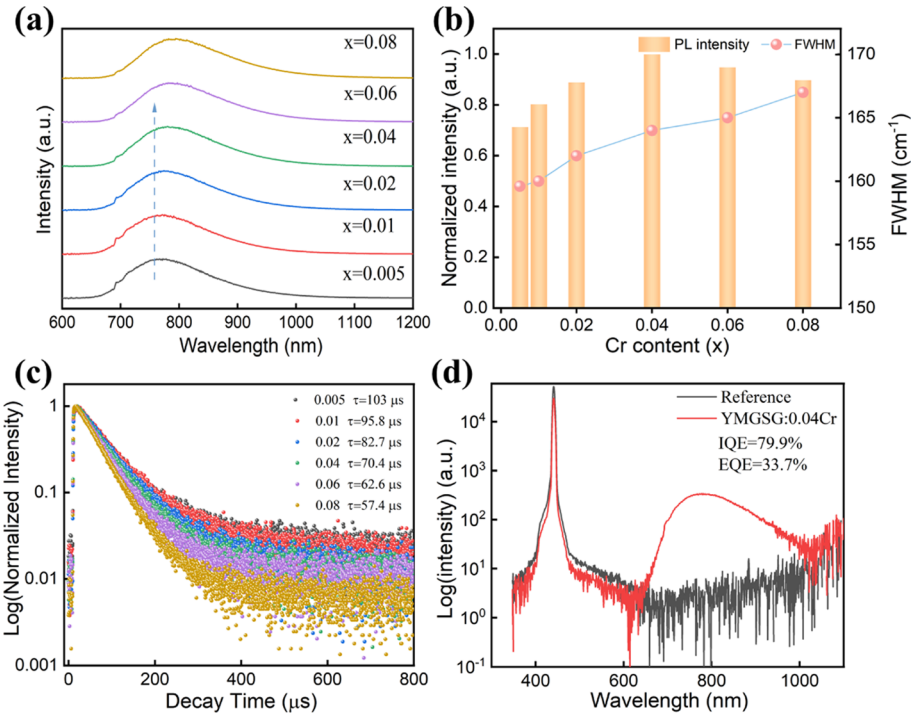

Figure 3. (a) Emission spectra, (b) PL intensity, FWHM and (c) decay times of YMGSG: xCr^{3+} (x = 0.005, 0.01, 0.02, 0.04, 0.06, 0.08). (d) IQE and EQE of YMGSG: 0.04Cr^{3+}.

elemental mapping of YMGSG: 0.04Cr^{3+} are depicted in Figure 1d. The phosphor shows irregular shape, and the particle size is about 3 μm. All elements are uniformly distributed on the particle surface.

3.2. Photoluminescence Properties. Figure 2a illustrates the DR, PLE, and PL spectra of YMGSG: 0.04Cr^{3+}. The DR spectrum shows two significant absorption bands at 438 and 622 nm, which corresponds to the $^4A_{2g} \rightarrow {}^4T_{1g}$ and $^4A_{2g} \rightarrow {}^4T_{2g}$ transitions of Cr^{3+} of PLE spectra, respectively. In the PLE spectrum, the positions of the excitation peaks are consistent with the absorption peaks in the DR spectrum. The sample emits a broadband spectrum (FWHM = 162 nm) centered at 782 nm after being excited by 438 nm light. The broadband NIR emission is derived from the $^4T_{2g} \rightarrow {}^4A_{2g}$ transition of Cr^{3+} in the weak octahedral CF. In addition, a weak sharp line emission peak at 696 nm caused by ^2E_g–$^4A_{2g}$ transition can be detected in all spectra.

The energy level diagram of Cr^{3+} ions with octahedral coordination can be well expressed by Tanabe−Sugano (Figure 2b).[32] The spectral properties of Cr^{3+} are intensely affected by the intensity of the CF, and it can be determined by the CF strength Dq and Racah parameter B (eq 1).[28,33,34]

$$10 \cdot D_q = E_a(_{2g})$$

$$\frac{D_q}{B} = \frac{15 \cdot (x - 8)}{x^2 - 10 \cdot x}$$

$$D_q \cdot x = E_a(4T_{1g}) - E_a(^4T_{2g}) \quad (1)$$

where $E_a(4T_{1g})$ and $E_a(^4T_{2g})$ stand for the energy positions of $4T_{1g}$ and $4T_{2g}$. The relationship between Stokes shift and bandwidth was also considered, and $E_a(_{2g})$ was determined as the average of the peak energies of the $^4A_{2g} \rightarrow {}^4T_{2g}$ excitation band and $^4T_{2g} \rightarrow {}^4A_{2g}$ emission band in this work. It is generally considered as a strong CF when $Dq/B > 2.3$, and a weak CF when $Dq/B < 2.3$. As shown in Figure 2b, when $Dq/B < 2.3$, the $^4T_2$ level lies in the lowest excited state. The $^4T_2$ and $^4A_2$ energy levels have different electronic configurations, and the $^4T_2$ energy level is strongly coupled to the host lattice,

https://doi.org/10.1021/acs.inorgchem.2c04319
Inorg. Chem. 2023, 62, 4220−4226

Table 2. PL Properties of Cr^{3+} Doped NIR Phosphors

phosphors	λ_{em} (nm)	I_{423K} (%)	FWHM (nm)	IQE (%)	EQE (%)	refs
Y3Ga3MgSiO12: Cr	782	84.4	162	79.9	33.7	this work
Ca2LuZr2Al3O12: Cr	780	60	117	69.1	31.5	29
$Ca_3Sc2Si3O12$: Cr	770	97.4	100	92.3	25.5	40
$Gd_3Zn_{0.8}Ga_{3.4}Ge_{0.8}O_{12}$: Cr	800	40.2	202	79.6	31.2	1
CaLu2Mg2Si3O12: Cr	755	92.1	120	48.5	20.7	25
$Gd_3Sc_{1.5}Al_0.5Ga3O12$: Cr	756	86	120	91		41
$KGaP_2O_7$: Cr	815	56	127	74.4	33.3	42
$LiInSi_2O_6$: Cr	840	77	143	75		23
AlP_3O9: Cr	780	91	120	76		20
CaMgGe2O6: Cr	845		160	84	30	39
Ca3Y2Ge3O12: Cr	800	<42%		81	10	43

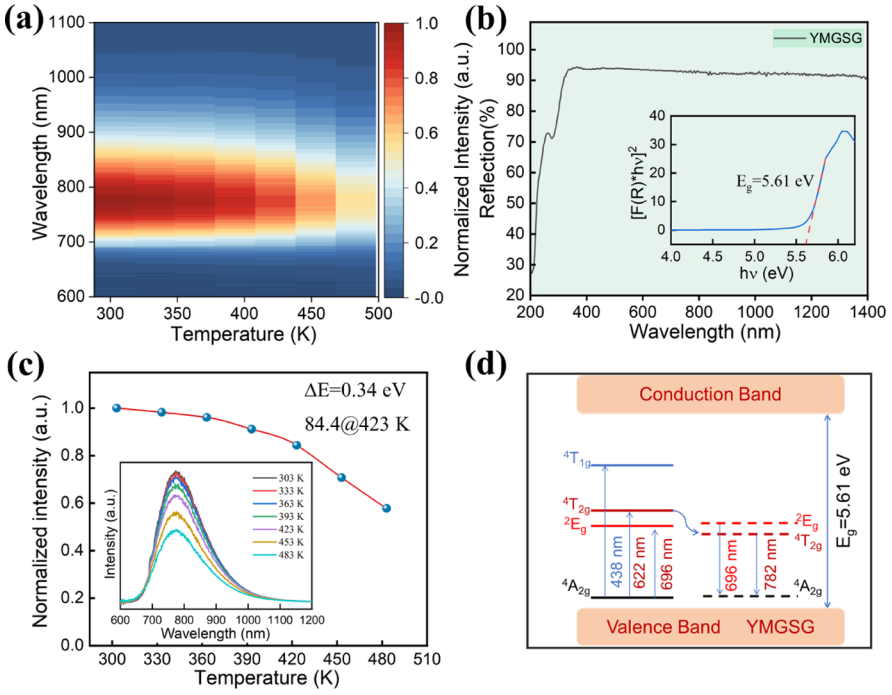

Figure 4. (a) Temperature dependent PL spectra of YMGSG: $0.04Cr^{3+}$ form 303 to 483 K. (b) DR spectra of YMGSG host and calculation value of the E_g. (c) Normalized total emission intensity versus the heating temperature. (d) Schematic diagrams of Cr^{3+} energy levels in the YMGSG host.

resulting in spin-allowed broadband emission of $^4T_2 \rightarrow {}^4A_2$ transition. The Dq/B of YMGSG: $0.04Cr^{3+}$ is calculated to be 2.01, which is smaller than 2.3. Thereby the transition of $^4T_2 \rightarrow {}^4A_2$ shows a broadband emission.

The normalized PLE spectra at different Cr^{3+} doping concentrations are given in Figure S1. The excitation peak positions changes slightly as the doping concentration increases, leading to the difficulty of determining the changes in CF by calculation. Figure 3a shows the PL spectra of YMGSG: xCr^{3+} (x = 0.005−0.08) phosphors excited by 438 nm. With increasing doping concentration, a redshift (~20 nm) of the emission spectrum was observed. The x = 0.04 sample exhibits the best PL intensity. In addition, the FWHM expands with increasing Cr^{3+} concentration, indicating the enhancement of the electron-lattice coupling effect (Figure 3b).

As we all know, Cr^{3+} (0.615 Å) prefers to occupy Ga(1)/Mg (0.62/0.72 Å) in octahedral position. The substitution of either Ga(1) or Mg will lead to lattice shrinkage, thus resulting in an increase in the CF intensity with increasing Cr^{3+} concentration, which is contradicted with the redshift of the PL spectra. This phenomenon also occurs in the Cr^{3+}-doped $Y_3In_{2-x}Ga_3O_{12}$ phosphor.[35] This is mainly attributed to the fact that the formation of Cr^{3+}−Cr^{3+} ion pairs will induce energy level splitting with increasing Cr^{3+} concentration, then leads to a redshift in the PL spectra. In addition, energy transfer between Cr^{3+} ions and Stokes shift could also lead to a non-negligible spectral redshift of the luminescent material.[36−38] With increasing Cr^{3+} concentration, the monitored decay lifetime decreases gradually from 103 to 57.4 μs, which is mainly caused by the concentration quenching.[35,39]

Figure 3d shows the IQE and EQE of YMGSG: $0.04Cr^{3+}$. The IQE of YMGSG: $0.04Cr^{3+}$ is 79.9%. The EQE is calculated to be 33.7%, which is better than most NIR phosphors reported in recent years (Table 2); the calculation process can be found in equation S1−S5 in Supporting Information. After doping with Mg−Si, octahedra undergo expansion, while tetrahedra appear to shrink (Figure S2). Thus, the high absorption efficiency may be caused by the

https://doi.org/10.1021/acs.inorgchem.2c04319
Inorg. Chem. 2023, 62, 4220−4226

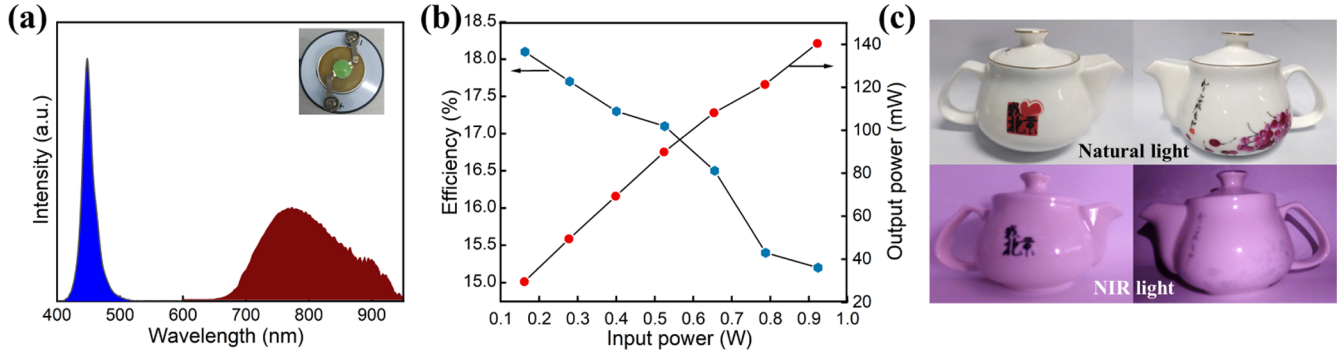

Figure 5. (a) Electroluminescence spectra of the NIR-pc-LED fabrited by YMGSG: 0.04Cr^{3+}. (b) Output power and photoelectric conversion efficiency versus input power. (c) Teapot photos in natural and NIR light.

distortion around the Ga1 site to break the parity-forbidden transition of Cr^{3+}.[34]

3.3. Temperature-Dependent Luminescence. Figure 4a shows a contour map of the temperature dependent emission spectra over the temperature range 303−483 K. The integrated emitting intensity decreases gradually as the temperature increases, and the integrated emitting intensity of YMGSG: 0.04Cr^{3+} still maintains 84.4% of that at room temperature (303 K) when heated to 423 K (Figure 4c). Compared with some recently reported Cr^{3+}-activated garnet NIR phosphors, YMGSG: 0.04Cr^{3+} shows comparable thermal stability (Table 2).

The thermal quenching behavior of phosphors is closely related to the electron-phonon coupling, band gap of host, and so forth.[35] The spectral profile (shape, FWHM, and peak wavelength) of the emission spectrum remains almost constant with increasing temperature (Figure S3). This indicates that its electron-phonon coupling effect is extremely weak. In addition, a common index for assessing the thermal stability of phosphors is activation energy (ΔE), which can be calculated by Arrhenius equation (Equation S6)[44,45] The ΔE of YMGSG: 0.04Cr^{3+} is calculated to be 0.34 eV (Figure S4), which is slightly larger than the value of $CaLu_2Mg_2Si_3O_{12}$: Cr^{3+}[29] (0.322 eV) and $Ca_3Sc_2Si_3O_{12}$: Cr^{3+}[40] (0.336 eV), implying its good thermal stability. Moreover, the band gap of the YMSGS host is calculated as 5.61 eV by the DR spectrum (Figure 4b). This value is much larger than that of most Cr^{3+} activated NIR garnet phosphors, such as $CaLu_2Mg_2Si_3O_{12}$: Cr^{3+} (5.17 eV),[25] $Y_3In_2Ga_3O_{12}$: Cr^{3+} (4.98 eV),[35] and $Gd_{2.4}Lu_{0.6}Ga_4AlO_{12}$: Cr^{3+} (4.34 eV).[36] Such a wide band gap ensures that the $^4T_{1g}$ and $^4T_{2g}$ energy levels are farther away from the conduction band (Figure 4d), thus suppressing the thermal ionization process and nonradiative relaxation.[25]

3.4. NIR-pc-LED Lamp Fabrication. To demonstrate the application of YMGSG: 0.04Cr^{3+} in NIR light sources, we fabricate a NIR-pc-LED device using the prepared phosphors packaged with blue LEDs. Figure 5a displays the electroluminescence spectra of the devices. Figure 5b presents the output power and photoelectric conversion efficiency against input power. The NIR output power increases with increasing input power, while the photoelectric conversion efficiency decreases gradually. The decrease in photoelectric conversion efficiency is attributed to the decreasing efficiency of the blue LED.[41] When the input power is 525 mW (2.92 V, 180 mA), the NIR output power and the photoelectric efficiency of the NIR pc LED are ∼89.8 mW and 17.1%, respectively. The NIR output power and photoelectric conversion efficiency of the NIR pc LED are better than most previously reported photovoltaic performance of Cr^{3+}-doped garnet phosphors (Table S2). Figure 5c demonstrates the application of the as prepared NIR light source for imaging. The NIR camera captures the shape of the teapot and the characters on it when illuminated by the NIR light source. The red logo turns black-and-white because it is out of the NIR camera's acceptance range. These results indicate that the developed YMGSG: 0.04Cr^{3+} phosphor is a promising candidate material for NIR-pc-LEDs.

4. CONCLUSIONS

To summarize, we report a newly developed, high-efficiency, thermally stable YMGSG: Cr^{3+} phosphor with broadband NIR emission. The phosphor emits a broadband spectrum (FWHM = 162 nm) centered at 782 nm after being excited by 438 nm light. Benefiting from the large band gap and the weak coupling of Cr^{3+} with the YMGSG matrix, the optimized YMGSG: 0.04Cr^{3+} shows a good thermal stability (84.4%@423 K). Meanwhile, owing to the high blue light absorption efficiency (42.2%), it leads to a high EQE of 33.7% for YMGSG: 0.04Cr^{3+}. Finally, we fabricate the NIR-pc-LEDs using the as-prepared phosphor and evaluate its performance. The NIR output power and photoelectric conversion efficiency of the lamp are as high as 89.8 mW and 17.1% at an input power of 525 mW, demonstrating that it is a promising candidate phosphor for broadband NIR-pc-LEDs.

■ ASSOCIATED CONTENT

Supporting Information

The Supporting Information is available free of charge at https://pubs.acs.org/doi/10.1021/acs.inorgchem.2c04319.

Normalized spectra of YMGSG: xCr^{3+} as a function of Cr^{3+} concentration; coordination environment of octahedra and tetrahedra before and after doping with Mg−Si; temperature dependent PL spectra of YMGSG: 0.04Cr^{3+} form 303 to 483 K; linear fitting $\ln\left(\frac{I_0}{I_T} - 1\right)$ *versus* $1/KT$ of YMGSG: 0.04Cr^{3+}; atomic parameters obtained from Rietveld refinement of YMGSG: 0.04Cr^{3+}; NIR pc-LED device parameters; calculation of EQE and absorption efficiency; and calculation of activation energy (PDF)

https://doi.org/10.1021/acs.inorgchem.2c04319
Inorg. Chem. 2023, 62, 4220−4226

AUTHOR INFORMATION

Corresponding Authors

Xue Jiang − *Beijing Advanced Innovation Center for Materials Genome Engineering, Corrosion and Protection Center, University of Science and Technology Beijing, Beijing 100083, China*; Email: jiangxue@ustb.edu.cn

Yanjing Su − *Beijing Advanced Innovation Center for Materials Genome Engineering, Corrosion and Protection Center, University of Science and Technology Beijing, Beijing 100083, China*; orcid.org/0000-0003-2773-4015; Email: yjsu@ustb.edu.cn

Authors

Lipeng Jiang − *Beijing Advanced Innovation Center for Materials Genome Engineering, Corrosion and Protection Center, University of Science and Technology Beijing, Beijing 100083, China*

Liangliang Zhang − *State Key Laboratory of Luminescence and Applications, Changchun Institute of Optics, Fine Mechanics and Physics, Chinese Academy of Sciences, Changchun 130033, China*; orcid.org/0000-0002-9546-8786

Quansheng Liu − *School of Materials Science and Engineering, Changchun University of Science and Technology, Changchun 130022, China*; orcid.org/0000-0002-8526-9214

Xiaoyun Mi − *School of Materials Science and Engineering, Changchun University of Science and Technology, Changchun 130022, China*

Zhan Yu − *Zhongguancun Key Laboratory of Solid-State Lighting, Beijing 100083, China*

Guocai Lv − *Basic Experimental Center of Natural Science, University of Science and Technology Beijing, Beijing 100083, China*

Complete contact information is available at: https://pubs.acs.org/10.1021/acs.inorgchem.2c04319

Notes

The authors declare no competing financial interest.

ACKNOWLEDGMENTS

This work was financially supported by the National Key Research and Development Program of China (2021YFB3501501), Guangdong Province Key Area R&D Program (2019B010940001).

REFERENCES

(1) Wang, Y.; Wang, Z.; Wei, G.; Yang, Y.; He, S.; Li, J.; Shi, Y.; Li, R.; Zhang, J.; Li, P. Ultra-Broadband and high efficiency Near-Infrared Gd3Zn Ga5-2Ge O12:Cr3+ (x = 0-2.0) garnet phosphors via crystal field engineering. *Chem. Eng. J.* **2022**, *437*, 135346.

(2) Yan, Y.; Shang, M.; Huang, S.; Wang, Y.; Sun, Y.; Dang, P.; Lin, J. Photoluminescence Properties of AScSi2O6:Cr3+ (A = Na and Li) Phosphors with High Efficiency and Thermal Stability for Near-Infrared Phosphor-Converted Light-Emitting Diode Light Sources. *ACS Appl. Mater. Interfaces* **2022**, *14*, 8179−8190.

(3) Lin, J.; Zhou, L.; Ren, L.; Shen, Y.; Chen, Y.; Fu, J.; Lei, L.; Ye, R.; Deng, D.; Xu, S. Broadband near-infrared emitting Sr3Sc4O9: Cr3+ phosphors: Luminescence properties and application in light-emitting diodes. *J. Alloys Compd.* **2022**, *908*, 164582.

(4) Jiang, H.; Chen, L.; Zheng, G.; Luo, Z.; Wu, X.; Liu, Z.; Li, R.; Liu, Y.; Sun, P.; Jiang, J. Ultra-Efficient GAGG:Cr 3+ Ceramic Phosphor-Converted Laser Diode: A Promising High-Power Compact Near-Infrared Light Source Enabling Clear Imaging. *Adv. Opt. Mater.* **2022**, *10*, 2102741.

(5) Fang, L.; Hao, Z.; Zhang, L.; Wu, H.; Wu, H.; Pan, G.; Zhang, J. Cr3+-doped broadband near infrared diopside phosphor for NIR pc-LED. *Mater. Res. Bull.* **2022**, *149*, 111725.

(6) Zhao, M.; Liu, S.; Cai, H.; Zhao, F.; Song, Z.; Liu, Q. Cr3+-Doped double perovskite antimonates: efficient and tunable phosphors from NIR-I to NIR-II. *Inorg. Chem. Front.* **2022**, *9*, 4602−4607.

(7) Zheng, G.; Xiao, W.; Wu, H.; Wu, J.; Liu, X.; Qiu, J. Near-Unity and Zero-Thermal-Quenching Far-Red-Emitting Composite Ceramics via Pressureless Glass Crystallization. *Laser Photon. Rev.* **2021**, *15*, 2100060.

(8) Lu, C.-H.; Tsai, Y.-T.; Tsai, T.-L.; Chan, T.-S.; Zhang, X.; Lin, C. C. Cr3+-Sphere Effect on the Whitlockite-Type NIR Phosphor Sr9Sc(PO4)7 with High Heat Dissipation for Digital Medical Applications. *Inorg. Chem.* **2022**, *61*, 2530−2537.

(9) Sun, X.; Li, J.; Feng, K.; Zheng, R.; Yuan, H. Luminescence characteristics of Bi3+, Cr3+ and Bi3+/Cr3+ activated Sr3Y2Ge3O12 phosphors. *J. Lumin.* **2022**, *248*, 118984.

(10) Wang, Y.; Wang, Z.; Wei, G.; Yang, Y.; He, S.; Li, J.; Shi, Y.; Li, R.; Zhang, J.; Li, P. Highly Efficient and Stable Near-Infrared Broadband Garnet Phosphor for Multifunctional Phosphor-Converted Light-Emitting Diodes. *Adv. Opt. Mater.* **2022**, *10*, 2200415.

(11) Zhong, C.; Zhang, L.; Xu, Y.; Wu, X.; Yin, S.; Zhang, X.; You, H. Novel broadband near-infrared emitting phosphor LiGe2(PO4)-3:Cr3+ with tuning and enhancement of NIR emission by codoping Sb5+. *J. Alloys Compd.* **2022**, *903*, 163945.

(12) Jiang, L.; Jiang, X.; Zhang, Y.; Wang, C.; Liu, P.; Lv, G.; Su, Y. Multiobjective Machine Learning-Assisted Discovery of a Novel Cyan-Green Garnet: Ce Phosphors with Excellent Thermal Stability. *ACS Appl. Mater. Interfaces* **2022**, *14*, 15426−15436.

(13) Jiang, L.; Jiang, X.; Lv, G.; Su, Y. A mini review of machine learning in inorganic phosphors. *J. Mater. Inf.* **2022**, *2*, 14.

(14) Xiang, J.; Zheng, J.; Zhao, X.; Zhou, X.; Chen, C.; Jin, M.; Guo, C. Synthesis of broadband NIR garnet phosphor Ca4ZrGe3O12: Cr3+, Yb3+ for NIR pc-LED applications. *Mater. Chem. Front.* **2022**, *6*, 440−449.

(15) Jiang, L.; Jiang, X.; Xie, J.; Sun, H.; Zhang, L.; Liu, X.; Bai, Z.; Lv, G.; Su, Y. Ultra-broadband near-infrared Gd3MgScGa2SiO12: Cr, Yb phosphors: Photoluminescence properties and LED applications. *J. Alloys Compd.* **2022**, *920*, 165912.

(16) Liu, S.; Wang, Z.; Cai, H.; Song, Z.; Liu, Q. Highly efficient near-infrared phosphor LaMgGa11O19:Cr3+. *Inorg. Chem. Front.* **2020**, *7*, 1467−1473.

(17) Yao, L.; Shao, Q.; Shi, M.; Shang, T.; Dong, Y.; Liang, C.; He, J.; Jiang, J. Efficient Ultra-Broadband Ga 4 GeO 8 :Cr 3+ Phosphors with Tunable Peak Wavelengths from 835 to 980 nm for NIR pc-LED Application. *Adv. Opt. Mater.* **2022**, *10*, 2102229.

(18) Yu, S.; Wei, Z.; Wu, J.; Wang, T.; Zhang, J.; Luo, X.; Li, Y.; Wang, C.; Zhao, L. Design and tuning Cr3+-doped near-infrared phosphors for multifunctional applications via crystal field engineering. *Dalton Trans.* **2022**, *51*, 2313−2322.

(19) Zhang, Q.; Liu, D.; Dang, P.; Lian, H.; Li, G.; Lin, J. Two Selective Sites Control of Cr 3+ -Doped ABO 4 Phosphors for Tuning Ultra-Broadband Near-Infrared Photoluminescence and Multi-Applications. *Laser Photon. Rev.* **2022**, *16*, 2100459.

(20) Huang, D.; Zhu, H.; Deng, Z.; Yang, H.; Hu, J.; Liang, S.; Chen, D.; Ma, E.; Guo, W. A highly efficient and thermally stable broadband Cr3+-activated double borate phosphor for near-infrared light-emitting diodes. *J. Mater. Chem. C* **2021**, *9*, 164−172.

(21) Zeng, H.; Zhou, T.; Wang, L.; Xie, R.-J. Two-Site Occupation for Exploring Ultra-Broadband Near-Infrared Phosphor-Double-Perovskite La2MgZrO6:Cr3+. *Chem. Mater.* **2019**, *31*, 5245−5253.

(22) Zhang, H.; Zhong, J.; Du, F.; Chen, L.; Zhang, X.; Mu, Z.; Zhao, W. Efficient and Thermally Stable Broad-Band Near-Infrared Emission in a $KAlP_2O_7:Cr^{3+}$ Phosphor for Nondestructive Examination. *ACS Appl. Mater. Interfaces* **2022**, *14*, 11663.

(23) Xu, X.; Shao, Q.; Yao, L.; Dong, Y.; Jiang, J. Highly efficient and thermally stable Cr3+-activated silicate phosphors for broadband near-infrared LED applications. *Chem. Eng. J.* **2020**, *383*, 123108.

(24) Jiang, L.; Jiang, X.; Xie, J.; Zheng, T.; Lv, G.; Su, Y. Structural induced tunable NIR luminescence of (Y,Lu)3(Mg,Al)2(Al,Si)3O12: Cr3+ phosphors. *J. Lumin.* **2022**, *247*, 118911.
(25) Li, R.; Liu, Y.; Yuan, C.; Leniec, G.; Miao, L.; Sun, P.; Liu, Z.; Luo, Z.; Dong, R.; Jiang, J. Thermally Stable CaLu 2 Mg 2 Si 3 O 12 :Cr 3+ Phosphors for NIR LEDs. *Adv. Opt. Mater.* **2021**, *9*, 2100388.
(26) Basore, E. T.; Wu, H.; Xiao, W.; Zheng, G.; Liu, X.; Qiu, J. High-Power Broadband NIR LEDs Enabled by Highly Efficient Blue-to-NIR Conversion. *Adv. Opt. Mater.* **2021**, *9*, 2001660.
(27) Zhao, F.; Song, Z.; Liu, Q. *Advances in Chromium-Activated Phosphors for Near-Infrared Light Sources*; Laser Photonics Rev., 2022; p 2200380.
(28) Zhang, L.; Wang, D.; Hao, Z.; Zhang, X.; Pan, G.-h.; Wu, H.; Zhang, J. Cr 3+ -Doped Broadband NIR Garnet Phosphor with Enhanced Luminescence and its Application in NIR Spectroscopy. *Adv. Opt. Mater.* **2019**, *7*, 1900185.
(29) Zhang, L.; Zhang, S.; Hao, Z.; Zhang, X.; Pan, G.-h.; Luo, Y.; Wu, H.; Zhang, J. A high efficiency broad-band near-infrared Ca2LuZr2Al3O12:Cr3+ garnet phosphor for blue LED chips. *J. Mater. Chem. C* **2018**, *6*, 4967−4976.
(30) Yuan, C.; Li, R.; Liu, Y.; Zhang, L.; Zhang, J.; Leniec, G.; Sun, P.; Liu, Z.; Luo, Z.; Dong, R.; et al. Efficient and Broadband LiGaP 2 O 7 :Cr 3+ Phosphors for Smart Near-Infrared Light-Emitting Diodes. *Laser Photon. Rev.* **2021**, *15*, 2100227.
(31) Jin, Y.; Zhou, Z.; Ran, R.; Tan, S.; Liu, Y.; Zheng, J.; Xiang, G.; Ma, L.; Wang, X.-j. Broadband NIR Phosphor Ca 2 LuScAl 2 Si 2 O 12 :Cr 3+ for NIR LED Applications. *Adv. Opt. Mater.* **2022**, *10*, 2202049.
(32) Zhao, M.; Liu, S.; Cai, H.; Zhao, F.; Song, Z.; Liu, Q. Efficient broadband near-infrared phosphor Sr2ScSbO6:Cr3+ for solar-like lighting. *Sci. China Mater.* **2022**, *65*, 748−756.
(33) Struve, B.; Huber, G. The effect of the crystal field strength on the optical spectra of Cr3+ in gallium garnet laser crystals. *Appl. Phys. B* **1985**, *36*, 195−201.
(34) Xiao, H.; Zhang, J.; Zhang, L.; Wu, H.; Wu, H.; Pan, G.; Liu, F.; Zhang, J. Cr 3+ Activated Garnet Phosphor with Efficient Blue to Far-Red Conversion for pc-LED. *Adv. Opt. Mater.* **2021**, *9*, 2101134.
(35) Li, C.; Zhong, J. Highly Efficient Broadband Near-Infrared Luminescence with Zero-Thermal-Quenching in Garnet Y3In2-Ga3O12:Cr3+ Phosphors. *Chem. Mater.* **2022**, *34*, 8418−8426.
(36) Zou, X.; Wang, X.; Zhang, H.; Kang, Y.; Yang, X.; Zhang, X.; Molokeev, M. S.; Lei, B. A highly efficient and suitable spectral profile Cr3+-doped garnet near-infrared emitting phosphor for regulating photomorphogenesis of plants. *Chem. Eng. J.* **2022**, *428*, 132003.
(37) Zhou, Y.; Zhuang, W.; Hu, Y.; Liu, R.; Jiang, Z.; Liu, Y.; Li, Y.; Zheng, Y.; Chen, L.; Zhong, J. A broad-band orange-yellow-emitting Lu2Mg2Al2Si2O12: Ce3+ phosphor for application in warm white light-emitting diodes. *RSC Adv.* **2017**, *7*, 46713−46720.
(38) Jiang, L.; Jiang, X.; Wang, C.; Liu, P.; Zhang, Y.; Lv, G.; Lookman, T.; Su, Y. Rapid Discovery of Efficient Long-Wavelength Emission Garnet:Cr NIR Phosphors via Multi-Objective Optimization. *ACS Appl. Mater. Interfaces* **2022**, *14*, 52124−52133.
(39) Fang, L.; Zhang, L.; Wu, H.; Wu, H.; Pan, G.; Hao, Z.; Liu, F.; Zhang, J. Efficient Broadband Near-Infrared CaMgGe2O6:Cr3+ Phosphor for pc-LED. *Inorg. Chem.* **2022**, *61*, 8815−8822.
(40) Jia, Z.; Yuan, C.; Liu, Y.; Wang, X.-J.; Sun, P.; Wang, L.; Jiang, H.; Jiang, J. Strategies to approach high performance in Cr3+-doped phosphors for high-power NIR-LED light sources. *Light Sci. Appl.* **2020**, *9*, 86.
(41) Basore, E. T.; Xiao, W.; Liu, X.; Wu, J.; Qiu, J. Broadband Near-Infrared Garnet Phosphors with Near-Unity Internal Quantum Efficiency. *Adv. Opt. Mater.* **2020**, *8*, 2000296.
(42) Zhong, J.; Li, C.; Zhao, W.; You, S.; Brgoch, J. Accessing High-Power Near-Infrared Spectroscopy Using Cr3+-Substituted Metal Phosphate Phosphors. *Chem. Mater.* **2022**, *34*, 337−344.
(43) Mao, N.; Liu, S.; Song, Z.; Yu, Y.; Liu, Q. A broadband near-infrared phosphor Ca3Y2Ge3O12:Cr3+ with garnet structure. *J. Alloys Compd.* **2021**, *863*, 158699.
(44) Jiang, L.; Zhang, X.; Tang, H.; Zhu, S.; Li, Q.; Zhang, W.; Mi, X.; Lu, L.; Liu, X. A Mg2+-Ge4+ substituting strategy for optimizing color rendering index and luminescence of YAG: Ce3+ phosphors for white LEDs. *Mater. Res. Bull.* **2018**, *98*, 180−186.
(45) Zhang, Q.; Li, G.; Dang, P.; Liu, D.; Huang, D.; Lian, H.; Lin, J. Enhancing and tuning broadband near-infrared (NIR) photoluminescence properties in Cr3+-doped Ca2YHf2Al3O12 garnet phosphors via Ce3+/Yb3+-codoping for LED applications. *J. Mater. Chem. C* **2021**, *9*, 4815−4824.

https://doi.org/10.1021/acs.inorgchem.2c04319
Inorg. Chem. 2023, 62, 4220−4226